Ca^{2+}, Mg^{2+}, and Troponin I Inhibitory Peptide Binding to a Phe-154 to Trp Mutant of Chicken Skeletal Muscle Troponin C†

Murali Chandra, William D. McCubbin, Kim Oikawa, Cyril M. Kay, and Lawrence B. Smillie*

Medical Research Council Group in Protein Structure and Function, Department of Biochemistry, University of Alberta, Edmonton, Alberta, Canada T6G 2H7

Received August 23, 1993; Revised Manuscript Received December 20, 1993®

ABSTRACT: The effects of Ca^{2+}, Mg^{2+}, and troponin I (TnI) inhibitory peptide (I_p) binding on the spectral properties of a Phe-154 to Trp mutant (F154W) of chicken recombinant troponin C (rTnC) have been examined. Residue 154 is positioned in the final flanking helix H of metal binding site IV. Since there are no other Tyr or Trp residues in the protein, spectral properties can be unambiguously assigned. No significant differences in the far UV CD spectra of rTnC and F154W were observed in either the absence or presence of Ca^{2+}. When reconstituted into whole Tn the ATPase specific activities ($\pm Ca^{2+}$) of the troponin–tropomyosin–actomyosin subfragment 1 system were the same for both proteins. A 2-fold reduction in Ca^{2+} affinity of C domain sites III/IV but not of N domain sites I/II in isolated F154W is explicable in terms of the environment of residue 154 in the relatively disordered apo-C domain and its buried position in the known ordered $2Ca^{2+}$ crystal structure. Filling of sites III/IV by divalent cations was accompanied by a number of spectral changes which were different for Ca^{2+} and Mg^{2+}. Binding of Ip peptides (residues 96–116 and 104–115(116)) elicited fluorescence emission spectral alterations in the presence of Ca^{2+}. These were not observed in its absence nor in the presence of Mg^{2+} even though binding occurs under these conditions. Since Ca^{2+} affinity to C domain but not to N domain sites was increased by Ip at the low concentrations of protein and Ip tested, Ip binding appears to be stronger with C domain. Binding affinity of I_p1 (TnI residues 96–116) was ~8-fold greater than for I_p2 (residues 104–116) or I_p3 (residues 104–115). We conclude that the binding interface between TnC and TnI involves TnI residues 96–103 in addition to 104–115 and that this interface is likely structurally different for the apo, $2Ca^{2+}$ and $2Mg^{2+}$ states.

Skeletal and cardiac muscle contraction and relaxation are regulated by the binding and release of Ca^{2+} to and from troponin C (TnC).[1] Conformational changes induced by Ca^{2+} are believed to be transmitted through the other members of the troponin complex, including troponin I (TnI), and T, to tropomyosin and actin, thus facilitating their interaction with myosin (for reviews, see Leavis & Gergely (1984), Zot & Potter (1987) and Grabarek et al. (1992)). Elucidation of the crystal structure of TnC has revealed a dumbbell-shaped molecule with two globular domains connected by an exposed α-helix (Herzberg & James (1985a,b, 1988), Herzberg et al. (1986), Strynadka & James (1989), Sundaralingam et al. (1985), Satyshur et al. (1988)). Each of the four metal-binding sites, I and II in the N domain and III and IV in the C domain, are arranged in the helix–loop–helix motif common to this class of proteins. Sites III and IV have a high affinity for Ca^{2+} ($K_a \cong 10^7\ M^{-1}$) and also bind Mg^{2+} ($K_a \cong 10^3\ M^{-1}$). They are believed to be invariably occupied by Ca^{2+}/Mg^{2+} *in vivo* and to perform a structural role. The conformational changes associated with the binding of metal to the lower affinity ($K_a \cong 10^5$–$10^6\ M^{-1}$) Ca^{2+} specific sites I and II, on the other hand, are considered to fulfill the regulatory function.

In the crystals (grown at pH ≅ 5) on which the X-ray structural determination is based, N domain sites I and II are unoccupied by Ca^{2+} whereas sites III and IV are filled. We refer to this known structure as the $2Ca^{2+}$ state. On the basis of extensive similarities in amino acid sequence between N and C domains and on the assumption that the structure of the Ca^{2+} filled N domain would resemble that of the known C domain, Herzberg et al. (1986) proposed a model for the conformational transition to the $4Ca^{2+}$ state. The structural transition would involve a rearrangement of secondary structural elements such that helices B and C move as a unit relative to the N, A, and D helices. As a result, a number of nonpolar residues, either totally or partially inaccessible to solvent in the $2Ca^{2+}$ state, would become exposed on the surface of the protein to form a "hydrophobic patch" in the $4Ca^{2+}$ state. The fully Ca^{2+} loaded protein would now have two such nonpolar surfaces, one on each of the N and C domains and each associated with a constellation of negatively charged side chains. Present evidence suggests that both of these are involved in interaction with TnI (Grabarek et al., 1992).

Recently two spectral probe mutants, F29W and F105W, have been described for monitoring the metal-induced structural transitions of N and C domains, respectively (Pearlstone et al., 1992; Trigo-Gonzalez et al., 1992). These have been shown to be specific for their respective domains and not to be significantly influenced by metal-induced conformational events in the other domain. The usefulness of one of these (F29W) has been demonstrated by its application to the analysis of five additional mutants with increased Ca^{2+} affinity (Pearlstone et al., 1992). In the present paper, we report the preparation and characterization of another C domain spectral probe mutant, F154W. In the $2Ca^{2+}$ crystal structure this residue occurs in the final flanking H helix of Ca^{2+} binding site IV and together with Phe-102 of helix E and Phe-151 of helix H forms an aromatic cluster constituting a portion of the hydrophobic core of the C domain. As such, they are all largely buried and inaccessible to solvent. In the tertiary structure of the $2Ca^{2+}$ and $4Ca^{2+}$ states this constellation is close to one of the putative troponin-I binding sites on TnC.

† This study was supported by the Medical Research Council of Canada.
® Abstract published in *Advance ACS Abstracts*, February 15, 1994.

[1] Abbreviations: TnC, troponin C; rTnC, recombinant troponin C; TnI, troponin I; Ip, inhibitory peptide; EGTA, [ethylenebis(oxyethylenenitrilo)]tetraacetic acid; myosin S1, myosin subfragment 1.

0006-2960/94/0433-2961$04.50/0

EXPERIMENTAL PROCEDURES

Mutagenesis, Expression, and Purification of Proteins. Chemicals, enzymes, and expression and purification of recombinant fusion TnC and its cleavage with factor Xa to recombinant TnC (rTnC)[2] were as described before (Golosinska et al., 1991; Reinach & Karlsson, 1988).

Polymerase chain reaction technology was used for the preparation of the site-specific mutant as described by Ho et al. (1989). The base sequence of the 5′ outside primer was

GAAGGGGGATCCATCGAGGGTAGGATGGCG

and that for the 3′ outside primer

TCTAGAGGATCCCCGGGTACCGAGCTCGAA

The 5′ outside primer anneals to sequences at the 5′ end of the TnC coding sequence near the *Bam*HI site whereas the 3′ outside primer is complimentary to sequences downstream from the 3′ end of the coding sequence, just beyond the *Eco*RI site. The two inside primers, containing mismatched bases designed to introduce a Trp for Phe mutant at residue 154, were

primer 1:

ATTGACTTCGATGAG*TGG*CTGAAGATGATG

primer 2:

CTCCATCATCTTCAG*CCA*CTCATCGAAGTC

Polymerase chain reactions were performed in a Perkin-Elmer thermal cycle under conditions as described (Ho et al., 1989). Briefly, the DNA fragments were amplified by adding 1 μg of template DNA (*Bam*HI fragment from pTZ18R·TnC) to 500 ng of each primer in 100 μL of polymerase chain reaction buffer (10 mM Tris·HCl, pH 8.3, 1.5 mM $MgCl_2$, 0.01% gelatin, 200 μM each dNTP and 2.5 units of Taq polymerase). Each reaction was overlayered with 100 μL of mineral oil and subjected to 30 cycles of denaturation (1 min, 94 °C), annealing (1 min, 55 °C), and extension (1 min, 72 °C). Products were analyzed on a 1.5% agarose gel. Mutagenesis was performed by carrying out two separate reactions: reaction I contained 5′ outside primer and primer 2; reaction II was carried out with 3′ outside primer and primer 1. In this study reaction II failed to amplify the desired DNA fragment. The DNA fragment from reaction I was purified on a 1.5% agarose gel, added in 5-fold excess to single-stranded template DNA (pTZ18R·TnC) denatured at 94 °C for 1 min, annealed at room temperature for 3–5 min, and extended in the presence of 200 μM each of the four dNTPs and 5 units of Klenow polymerase for 4–6 h. Following transformation into JM109 *Escherichia coli* cells, the single-stranded DNA was isolated (Mead et al., 1986) from single colonies and sequenced to confirm the mutation. The *Eco*R1 fragment carrying the mutation was then ligated into the expression vector pLcII (Reinach & Karlsson, 1988).

TnI Inhibitory Peptides. Three inhibitory peptides, purchased from the Alberta Peptide Institute, were used in the present work. They corresponded to residues 96–116, 104–116, and 104–115 of the amino acid sequence of rabbit skeletal fast muscle TnI (Wilkinson & Grand, 1978). In the following they are designated Ip1, Ip2, and Ip3 and differ not only in length but also at their amino and carboxyl ends by the absence or presence of acetyl and amide groups, respectively.

	96	116
Ip1	NH_2-NQKLFDLRGKFKRPPLRRVRM-OH	
	104	116
Ip2	AcGKFKRPPLRRVRM-OH	
	104	115
Ip3	AcGKFKRPPLRRVR-NH_2	

Spectral Measurements. Precautionary measures taken for the preparation of buffer and protein solutions have been described (Golosinska et al., 1991). Protein and peptide concentrations were determined by amino acid analysis using norleucine as an internal standard. Final protein concentrations for each spectral measurement are given in the figure captions. Buffer conditions for all spectral measurements were 50 mM 3-(*N*-morpholino)propanesulfonic acid, 100 mM KCl, 1 mM EGTA, 1 mM DTT, pH 7.1. Far UV CD measurements, near UV CD spectra, difference UV absorbance spectra, and fluorescence titrations were essentially as previously described (Pearlstone et al., 1992). Fluorescence measurements with F154W were on a Perkin-Elmer MPF-44B recording fluorescence spectrophotometer attached to a microprocessor controlled differential corrected spectra unit (DCSU2) which allows for automatic fluorescence background correction. The instrument was operated in the ratio mode with 5-nm bandwidths for excitation and emission slits. Fluorescence measurements were at 90° to the source. Excitation was at 282 nm, and emission was recorded from 200 to 400 nm with the reference mode set on the DCSU2. Temperature was controlled at 20 °C with circulating water. Calcium titrations and calculation of free Ca^{2+} concentrations were as described before except that, for F154W, the log of the binding constant for F154W + 2Ca ⇌ F154W·2Ca was taken as 12.7.

Fluorescence quenching at 20 °C was measured at the emission maxima of the proteins and carried out by sequential addition of 5 μL of 8 M acrylamide to 1 mL initial volume of protein. Excitation was at 295 nm. Data were corrected for dilution and for acrylamide absorption using $F_{corr} = F \times 10^{A/2}$ where A is absorbance in a 1-cm cell at 295 nm and F the observed fluorescence. The corrected fluorescence quenching data were treated with a modified form of the Stern–Volmer equation (Eftink & Ghiron, 1976),

$$F_0/F = (1 + K_{SV}[Q]) \exp(V[Q])$$

where $\exp(V[Q])$ is the static quenching term, F_0 and F are observed fluorescence intensities in the absence and presence of quencher, Q; K_{SV} is the Stern–Volmer quenching constant; and V is the static quenching constant. The values listed in Table 2 were obtained by fitting the data to the above equation by a nonlinear least squares analysis program written for the Macintosh computer.

Troponin–Tropomyosin–Actomyosin Subfragment 1 ATPase Measurements. Proteins were prepared from rabbit back and leg muscle by established procedures: myosin subfragment 1 (S1) (Weeds & Taylor, 1975); actin (Spudich & Watt, 1971); tropomyosin (Smillie, 1982); TnI and troponin T (Mak et al., 1983). The reconstitution of whole troponin from its components was as described by Tobacman and Lee (1987) with one modification. Troponins C, I, and T were mixed at a molar ratio of 1.4:1:1 (instead of 1:1:1) in the presence of 4.6 M urea. In our experience, this higher concentration of TnC served to prevent protein precipitation in the subsequent

[2] The differences in amino acid sequences between chicken muscle TnC and the recombinant TnC have been described (Golosinska et al., 1991).

Table 1: Ca^{2+} Binding Parameters for rTnC and F154W in the Absence and Presence of Inhibitory Peptide Ip1

	low-affinity sites		high-affinity sites	
protein[a]	$-\log K_2$	n_2	$-\log K_1$	n_1
rTnC	5.55 (±0.08)	1.6 (±0.2)	6.62 (±0.01)	2.0 (±0.1)
rTnC + Ip1	5.66 (±0.07)	1.8 (±0.2)	7.12 (±0.05)	1.7 (±0.1)
F154W	5.50 (±0.06)	1.3 (±0.2)	6.35 (±0.04)	1.8 (±0.1)
F154W + Ip1	5.67 (±0.02)	1.5 (±0.2)	6.99 (±0.08)	2.0 (±0.1)
F154W			6.35 (±0.05)	1.8 (±0.1)
F154W + Ip1			6.99 (±0.05)	2.2 (±0.1)

[a] Data were obtained from Ca^{2+} titration of far UV CD (first four rows) and fluorescence emission (last two rows; see Figure 1A,B). The data from each titration were analyzed separately (Golosinska et al., 1991) to provide values for the apparent dissociation constants K_1 and K_2 and Hill coefficients n_1 and n_2. Deduced values of $-\log K$ and n from several titrations were averaged and are presented above with standard deviations in parentheses.

dialysis steps. In control experiments with rabbit skeletal TnC, this higher ratio of TnC to the other components did not affect Ca^{2+}-activated ATPase levels in the reconstituted troponin–tropomyosin–actomyosin S1 system. Final dialysis of the reconstituted troponin was against assay buffer (see below). Protein concentrations were based on amino acid analyses except for myosin S1, which was estimated by absorbance at 280 nm using $E_{1\%} = 7.9$. Final dialysis of stock solutions of all proteins was against assay buffer containing 20 mM imidazole, 6.5 mM KCl, 3.5 mM $MgCl_2$, 1 mM dithiothreitol, 0.5 mM EGTA, 0.01%, NaN_3, pH 7.0. For all assays the reaction at 25 °C included final concentrations of 0.3 μM myosin S1, 25 μM F-actin, 7.14 μM tropomyosin, and 7.14 μM troponin. Free Ca^{2+} concentration was adjusted to pCa values of 8.5 or 5.0 (where pCa ≡ $-\log [Ca^{2+}]_{free}$) by addition of appropriate aliquots of 5 mM $CaCl_2$. Values of pCa were calculated for 25 °C using the SPECS program of Fabiato (1988) and the association constants for Mg^{2+} and Ca^{2+} binding to EGTA and ATP adjusted for ionic strength as recommended by Tobacman (1987). Reactions were initiated by addition of 20 mM ATP in assay buffer to a final concentration of 1 mM in a total reaction volume of 0.3 mL. Release of inorganic phosphate was measured by the colorimetric method of Heinonen and Lahti (1981). Reactions were terminated after 20 min, well within the linear range of the progress curve even at the highest ATPase rates.

RESULTS

Effects of Ca^{2+} and Mg^{2+} on Spectral Properties of F154W. The far UV CD spectra of F154W in the presence and absence of Ca^{2+} were found to be very similar to those previously reported for rTnC (Pearlstone et al., 1992). In the apo and $4Ca^{2+}$ states the averaged $[\theta]_{221nm}$ values of 10 determinations were found to be −11 670 ± 500 and −17 550 ± 350 deg·cm²·dmol⁻¹, respectively. These can be compared with values of −11 160 ± 960 and −17 560 ± 800 deg·cm²·dmol⁻¹ for rTnC previously determined (Pearlstone et al., 1992). These values, in close agreement with those for rabbit skeletal muscle TnC (Johnston & Potter, 1978; McCubbin et al., 1982) and chicken skeletal muscle TnC (Golosinska et al., 1991) indicate that substitution of Phe-154 by Trp has had little effect on the overall secondary structure of the protein.

Calcium titration curves of the far UV [θ] at 221 nm of rTnC and F154W are shown in Figure 1A. For each set of averaged titration data, a curve was fitted by use of a nonlinear iterative least-squares procedure using an equation for two binding components as previously described (Golosinska et al., 1991). It was assumed that 73% of the total ellipticity

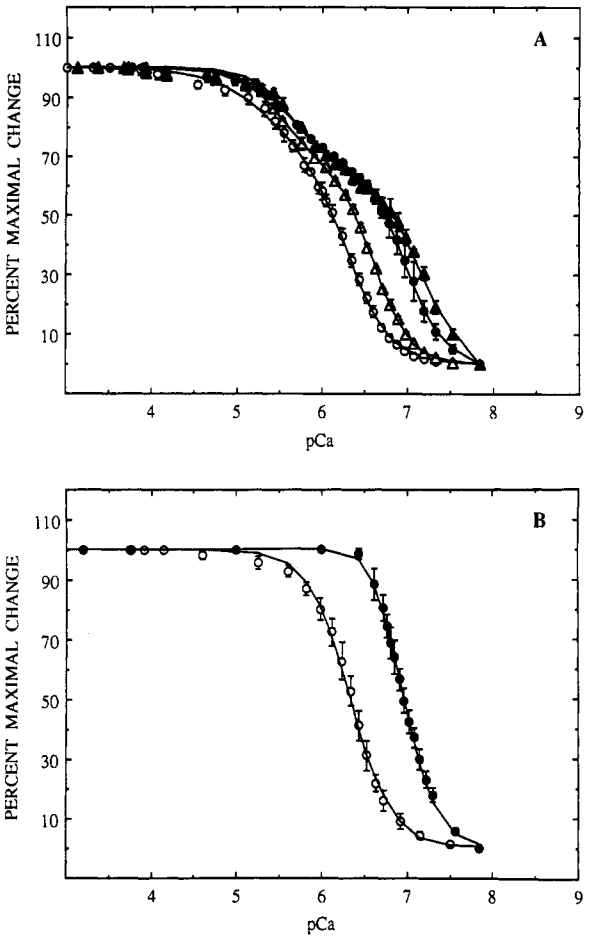

FIGURE 1: (A) Far UV CD Ca^{2+} titration curves in the presence and absence of TnI inhibitory peptide 96–116. The error bars represent the standard deviation of two experiments for each curve. The best fit for the data points was obtained as described (Pearlstone et al., 1992). rTnC (△), rTnC + Ip1 (▲), F154W (○), F154W + Ip1 (●). Protein concentration was 35 μM. The molar ratio of protein to Ip1 was 1:5. Ellipticity was measured at 221 nm. (B) Ca^{2+} titration curves of Trp fluorescence intensities of F154W in the presence and absence of Ip1. F154W (○), F154W + Ip1 (●). The error bars represent the standard deviation of at least four experiments. The best fit for the data was obtained as described (Pearlstone et al., 1992). Protein concentration was 3.8 μM. The molar ratio of F154W to Ip1 was 1:5.

change was contributed by the high-affinity domain (sites III and IV) and 27% by the low-affinity domain (sites I and II) (Li et al., 1994). The four parameters describing the biphasic curves for each of the two proteins are given in Table 1. The data indicate that the affinity of Ca^{2+} binding to the high-affinity sites of F154W has been reduced 2-fold. The differences for the $-\log K_2$ values of sites I/II of the N domain of the two proteins are within experimental error.

The Trp fluorescence emission spectra of F154W in the absence of metal ion and in the presence of Mg^{2+} and Ca^{2+} are shown in Figure 2A. When Ca^{2+} and Mg^{2+} are added, there is a blue shift in the λ_{max} from 343 nm to 318 nm in both cases, indicating that the conformational changes induced by Ca^{2+} or Mg^{2+} lead to a more nonpolar environment for Trp 154. The quantum yields are increased from 0.089 (apo) to 0.092 (Ca^{2+}) and 0.120 (Mg^{2+}), respectively. In these experiments a high concentration (40 mM) of Mg^{2+} was used to more completely saturate sites III/IV. This is necessary since, with $K_a \cong 4 \times 10^3$ M^{-1} (Potter & Gergely, 1975) and Mg^{2+} concentrations of 2–5 mM, there would be a low level of occupancy by Mg^{2+} at these sites. Control experiments at 2 and 5 mM Mg^{2+} (not shown) gave the same emission spectra

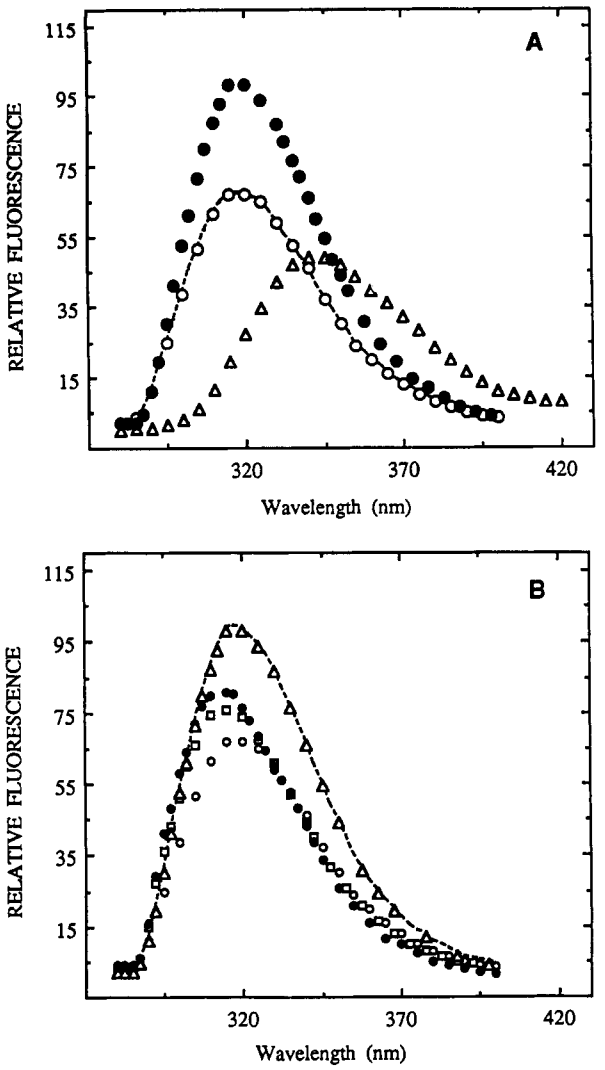

FIGURE 2: Emission fluorescence spectra of F154W in EGTA, Ca^{2+}, and Mg^{2+} and in complex with Ip1. (A) 1 mM EGTA (△), 2 mM Ca^{2+} (○), 40 mM Mg^{2+} (●), 40 mM Mg^{2+} + 2 mM Ca^{2+} (- - -). Excitation was at 282 nm. For quantum yield measurements, the data were normalized using a quantum yield of 0.13 for Trp. The quantum yields were as follows: apo, 0.089; Ca^{2+}, 0.092; Mg^{2+}, 0.12. (B) 2 mM Ca^{2+} (○), 2 mM Ca^{2+} + Ip1 (●), 2 mM Ca^{2+} + Ip1 + 40 mM Mg^{2+} (□), 40 mM Mg^{2+} (△), 40 mM Mg^{2+} + Ip1 (- - -). Protein concentration was 3.8 μM. The molar ratio of F154W to Ip1 was 1:5.

and λ_{max} as with 40 mM Mg^{2+} but with much lower quantum yields. Interestingly, the spectra for the plus Ca^{2+} and plus Ca^{2+} + Mg^{2+} situations are virtually superimposable and different from those for the plus Mg^{2+} state. Clearly Ca^{2+} (2 mM) displaces the Mg^{2+} (40 mM) from sites III and IV at these concentrations, as expected from the known binding constants (Potter & Gergely, 1975). The data also show that the high ionic strength contributed by 40 mM Mg^{2+} has minimal effect on the fluorescence emission of Ca^{2+}-saturated F154W. The differences in the emission spectra also show that the environment of Trp 154 is not identical in the plus Ca^{2+} and plus Mg^{2+} states. A similar observation has been made with the previously described C domain spectral probe mutant F105W (Trigo-Gonzalez et al., 1992).

The changes in metal induced fluorescence emission (monitored at 310 nm) as a function of free [Ca^{2+}] where pCa ≡ −log [Ca^{2+}] are shown in Figure 1B. The titration data could be fitted to an equation for one binding component (Golosinska et al., 1991) from which the values −log K_1 = 6.35 and a Hill coefficient of n = 1.8 were obtained (Table 1). These values are in good agreement with those derived from far UV CD analyses and are attributable to the C domain high-affinity sites III and IV. The observations therefore indicate that the fluorescence changes induced in F154W by Ca^{2+} are associated only with metal induced conformational transitions of the C domain. They also show again that the substitution of Phe-154 by Trp has reduced the Ca^{2+} affinity of sites III/IV 2-fold.

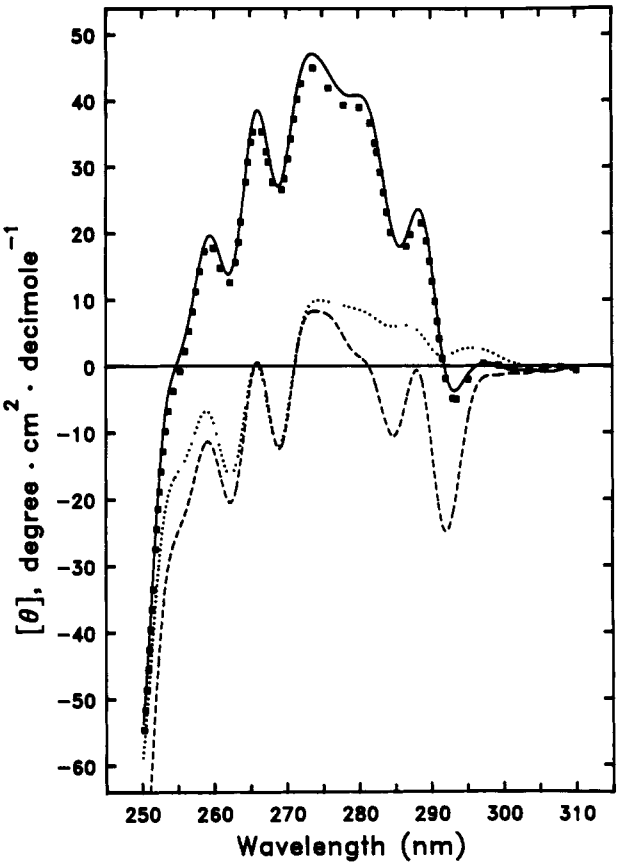

FIGURE 3: Near UV CD spectra of F154W in EGTA, Ca^{2+} and Mg^{2+} states: 1 mM EGTA (···), 2 mM Ca^{2+} (■), 2 mM Ca^{2+} + 40 mM Mg^{2+} (—), and 40 mM Mg^{2+} (- - -). Protein concentration was 71 μM.

The effects of the metal induced conformational transition on the environment of Trp-154 were also investigated by UV difference spectroscopy (not shown). Although the difference spectra induced by Ca^{2+} and Mg^{2+} were rather similar, the magnitudes of the peaks and troughs were different. Those for Mg^{2+} were shifted to slightly longer wavelengths.

The effects of Ca^{2+} and Mg^{2+} on the near UV CD spectrum of F154W are shown in Figure 3. Positive ellipticity between 280 and 290 nm for the apo protein is increased further in the presence of Ca^{2+} (2 mM) and decreased to negative values in the presence of Mg^{2+} (40 mM). Significantly, the further addition of Ca^{2+} (2 mM) to the 40 mM Mg^{2+} F154W solution gave a spectrum virtually identical to that seen in 2 mM $CaCl_2$ alone. These data further demonstrate that the environment of F154W is different when Ca^{2+} is bound to sites III/IV than when Mg^{2+} is bound and that these differences cannot be attributed to differences in ionic strength.

As a further measure of the accessibility of Trp-154 to solvent, the acrylamide quenching method was used to monitor differences in the apo, Ca^{2+}, and Mg^{2+} states of the protein. The data (see Figure 4A,B) were analyzed with the modified Stern–Volmer equation, and values for K_{SV}, the Stern–Volmer quenching constant, and V, the static quenching constant,

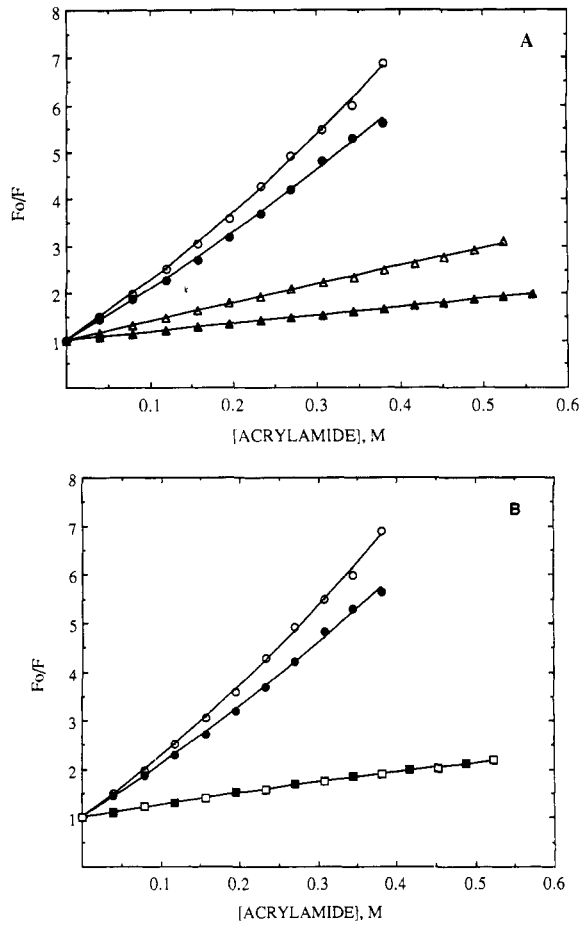

FIGURE 4: Acrylamide quenching of F154W TnC in 1 mM EGTA, 2 mM Ca^{2+}, and 40 mM Mg^{2+} and in complex with Ip1. (A) Effect of Ip1 in the presence and absence of Ca^{2+}. Apo F154W (○), apo F154W + Ip1 (●), F154W + Ca^{2+} (△), and F154W + Ca^{2+} + Ip1 (▲). (B) Effect of Ip1 in the presence and absence of Mg^{2+}. Apo F154W and Apo F154W + Ip1 are as shown in panel A. F154W + Mg^{2+} (□), F154W + Mg^{2+} + Ip1 (■). The concentrations of F154W and Ip1 were 4.48 and 22.5 μM, respectively.

Table 2: Stern–Volmer Constants Derived from Acrylamide Quenching of Fluorescence of F154W in the Absence and Presence of Ca^{2+}, Mg^{2+}, and Ip1[a]

	K_{SV} (M^{-1})	V (M^{-1})
F154W[b] + EGTA	11.55 (±0.42)	0.84 (±0.25)
F154W[b] + EGTA + Ip1	10.62 (±0.91)	0.39 (±0.24)
F154W[c] + Ca^{2+}	4.46 (±0.72)	0
F154W[d] + Ca^{2+} + Ip1	1.68 (±0.03)	0
F154W[c] + Mg^{2+}	3.12 (±0.01)	0
F154W[c] + Mg^{2+} + Ip1	3.03 (±0.12)	0

[a] K_{SV} and V were calculated as described in Experimental Procedures. The protein concentration was 4.5 μM and, when present, Ip1 was 22.5 μM. [b] Fluorescence was measured at 343 nm. [c] Fluorescence was measured at (318 nm). [d] Fluorescence was measured at 313 nm.

were derived (see Table 2). In those cases in which there is upward curvature in the F_0/F *vs* [acrylamide], the curves were linearized by assumption of an appropriate value for V in the term exp V[Q]. This was necessary for the apo state but unnecessary in the Ca^{2+} and Mg^{2+} states. In the latter two cases V was taken as 0. Taking the magnitude of the K_{SV} quenching constant as a measure of solvent accessibility to the side chain of Trp-154 (Table 2), it can be seen that this is much reduced in the presence of metal ion. Again there is a significant difference between the Ca^{2+} and Mg^{2+} states, with Trp-154 of the Mg^{2+} state being less accessible to quencher than that of the Ca^{2+} state.

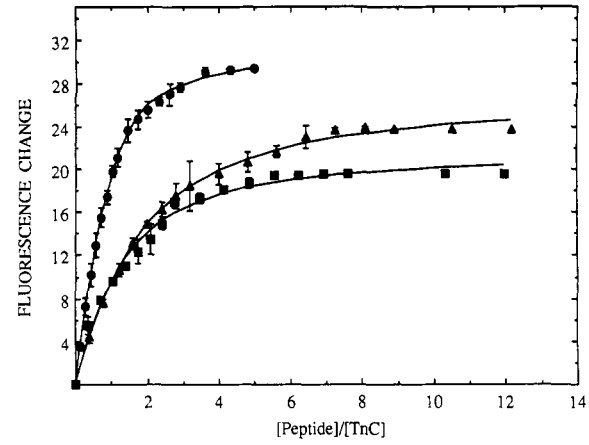

FIGURE 5: Titration of F154W in the presence of Ca^{2+} with TnI inhibitory peptides Ip1 (●), Ip2 (■), and Ip3 (▲) as monitored by Trp fluorescence. Titrations were performed in 50 mM MOPS, 100 mM KCl, 1 mM EGTA, 2 mM Ca^{2+}, 1 mM DTT, pH 7.1 buffer. Fluorescence emission was monitored at 310 nm. The data were fit to a simple 1:1 binding equation (see text) with association constants of 5.0 (±0.9) × 10^5, 6.5 (±1.6) × 10^4, and 6.3 (±2.6) × 10^4 M^{-1}, respectively. Protein concentration was 8.3 μM. Each curve is the average of at least three titrations.

Effects of Troponin I Inhibitory Peptide Binding on Spectral Properties of F154W. To examine the effects of Ip peptide binding to F154W on its Ca^{2+} affinity, the $[\theta]_{221nm}$ of mixtures of F124W or rTnC and Ip1 was monitored as a function of Ca^{2+}. A molar ratio of protein to Ip1 of 1:5 was used since the data shown subsequently (see Figure 5) demonstrated that this was adequate to saturate the protein with Ip1. The titration data are shown in Figure 1A, and the derived binding parameters are given in Table 1. The interaction of either rTnC or F154W with Ip1 is seen to increase the Ca^{2+} binding affinity of the C domain sites III/IV by a factor of about 3-fold or 4.5-fold, respectively. At these concentrations of protein and Ip1, there was minimal effect of Ip1 binding on the Ca^{2+} affinity of the N domain sites I/II. Similar Ca^{2+} titration of F154W in the presence of a 5-fold excess of Ip1 was monitored by fluorescence emission at 307 nm (Figure 1B). Fitting of the data to the equation for a single binding component gave a value of $-\log K_1$ of 6.99 (Table 1). This is in reasonable agreement with that deduced for F154W in the presence of Ip1 for the high-affinity sites III/IV from the far UV CD titration data (Figure 1A and Table 1).

To explore the potential for the application of the fluorescence properties of F154W to an investigation of the binding of TnI inhibitory peptides to the protein, the fluorescence emission spectra of F154W in the presence of Ip1 were examined under various ionic conditions. In the absence of metal ions or in the presence of 40 mM Mg^{2+}, the addition of Ip1 to a molar ratio of 5:1 (Ip1:F154W) had no effect on the fluorescence emission spectrum of the protein (Figure 2B). However, in the presence of 2 mM Ca^{2+}, Ip1 addition produced a small shift of λ_{max} from 318 nm to 313 nm and a significant increase in the fluorescence emission at the latter wavelength (Figure 2B). Addition of Ip1 in the presence of 40 mM Mg^{2+} and 2 mM Ca^{2+} produced a similar but slightly smaller increase. This smaller increase as compared with that in 2 mM Ca^{2+} alone (without Mg^{2+}) was shown to be an ionic strength effect since identical fluorescence emission spectra were obtained when 40 mM Mg^{2+} was substituted with 120 mM KCl (spectrum not shown). We attribute this ionic strength effect to a weakening of the interaction of Ip1 with the protein since no such effect was seen in the fluorescence

properties of F154W in Mg^{2+} plus Ca^{2+} conditions when compared with Ca^{2+} alone (see Figure 2A).

The fluorescence spectral changes observed when Ip1 is added to the Ca^{2+} charged state of F154W has enabled an investigation of the binding affinities of inhibitory peptides Ip1, Ip2, and Ip3. Titration data for each of these are illustrated in Figure 5. Binding constants were derived from a nonlinear least squares fit to the data assuming binary complex formation (Williams et al., 1985). For the three peptides Ip1, Ip2, and Ip3, these were calculated to be 5.0 ($\pm$0.9) $\times 10^5$, 6.5 ($\pm$1.6) $\times 10^4$, and 6.3 ($\pm$2.6) $\times 10^4$ M^{-1}, respectively.

The influence of Ca^{2+} and Mg^{2+} on the acrylamide fluorescence quenching of F154W described above was extended to include the effects of Ip1 (see Figure 4 and Table 2). Both the plotted data and the calculated K_{SV} values show that Ip1 reduces acrylamide quenching in the Ca^{2+} charged state of the protein. No effect was seen of the inhibitory peptide on the fluorescence quenching in the presence of Mg^{2+}, and the small effect observed for the apo state cannot be considered as statistically significant. These observations indicate that the side chain of Trp-154 becomes less exposed to solvent when Ip1 binds to the protein in the presence of Ca^{2+}.

Functionality of F154W in a Reconstituted Troponin–Tropomyosin–Actomyosin S1 ATPase System. In order to establish that the substitution of Phe-154 by Trp had no deleterious effect on the biological activity of the protein, the mutant's ability to function in a reconstituted Ca^{2+} regulated actomyosin S1 ATPase system was compared with that of rTnC. In the absence of Ca^{2+} (pCa = 8.5), the specific activities with rTnC and F154W were 0.03 $\pm$ 0.01 s^{-1} and 0.10 $\pm$ 0.03 s^{-1}, respectively. In the presence of Ca^{2+} (pCa = 5.0), these were increased to 2.69 $\pm$ 0.02 s^{-1} (rTnC) and 2.82 $\pm$ 0.07 s^{-1} (F154W). We conclude that mutation of Phe-154 to Trp has not adversely affected rTnC's functional capacity as assessed in this system.

DISCUSSION

Previously we (Pearlstone et al., 1992) and others (Trigo-Gonzalez et al., 1992) have shown that the substitution of a Phe residue by Trp in chicken skeletal muscle rTnC can serve as a useful spectral probe for monitoring metal induced conformational transitions of the molecule. These are particularly useful in this protein since chicken TnC is normally devoid of Tyr or Trp. Thus spectral features can be unambiguously assigned to the side chain of the single introduced Trp residue. For each of the two previously described mutants, F29W and F105W, the fluorescence changes associated with the divalent metal induced conformational changes could be correlated with the binding of Ca^{2+} and/or Mg^{2+} to N and C domains, respectively. No evidence was obtained for an effect of metal binding to one domain on the other.

In the present paper, we describe an additional Trp for Phe mutant, designated F154W. In the $2Ca^{2+}$ crystal structure and the postulated $4Ca^{2+}$ state, this residue occurs in the final flanking H helix of Ca^{2+} binding site IV and together with Phe-102 of helix E and Phe-151 of helix H forms an aromatic cluster constituting a portion of the hydrophobic core of the C domain. As such these residues are largely buried and relatively inaccessible to solvent. They are also close to the nonpolar surface of the protein's C domain implicated in binding to TnI.

The present data indicate that the substitution of Phe-154 by Trp has little effect on the overall secondary structural features of the protein as indicated by far UV CD measurements. This was true for both the zero Ca^{2+} and $4Ca^{2+}$ states in which there were no significant experimental differences between the far UV CD spectra and $[\theta]_{221nm}$ values of the rTnC and F154W proteins. These were also similar to those previously reported for rabbit skeletal muscle TnC (Johnson & Potter, 1978; McCubbin et al., 1982) and for F29W (Pearlstone et al., 1992). We have also shown that the rTnC and F154W proteins have the same biological activities as measured by their abilities to function in the Ca^{2+} regulation of the reconstituted troponin–tropomyosin–actomyosin S1 ATPase system.

Although the properties described above are not affected by the substitution of Phe-154 by Trp, Ca^{2+} titration of the isolated mutant demonstrates a significantly reduced affinity of C domain sites III and IV for Ca^{2+} as monitored by both far UV CD and fluorescence measurements. Thus the –log K_1 value of 6.62 for the rTnC is reduced to 6.35 for F154W. These values correspond to apparent association constants of 4.0×10^6 and 2.2×10^6 M^{-1}, respectively. Within experimental error, Ca^{2+} affinity to N domain sites I/II is not significantly affected (see Figure 1A and Table 1). This 2-fold reduction in Ca^{2+} affinity of the C domain sites in F154W is not unexpected in light of the nonpolar core position of the naturally occurring Phe residue in the known crystal structure of the protein. In this $2Ca^{2+}$ state, Phe-154 is completely buried and inaccessible to solvent and has multiple van der Waals contacts with neighboring residues. Although details of the structure of the apo state are unknown, its C domain is mostly disordered (see review by Leavis & Gergely (1984)). Phe-154 is thus likely to be largely exposed and accessible to solvent. Its substitution by Trp in the F154W mutant can be expected to have little influence on the stability of the apo state but, because of its larger side-chain volume, to have an at least local disruptive and destabilizing effect on the structure of the $2Ca^{2+}$ state. Consequently, the equilibrium would be shifted from the $2Ca^{2+}$ state toward the zero Ca^{2+} state, leading to a reduced Ca^{2+} affinity of C domain sites III/IV.

The several spectral features of the single Trp residue in F154W observed in the present work are consistent with its shielded nonpolar environment in the $2Ca^{2+}$ state and its more exposed solvent accessibility in the zero Ca^{2+} state. Thus, in the presence of Ca^{2+} the λ_{max} of its fluorescence emission spectrum is blue-shifted to 318 nm from 343 nm (Figure 2), its near UV CD spectrum in the 275–295-nm range becomes more positive (Figure 3), and fluorescence quenching by increasing concentrations of acrylamide is significantly reduced. These are all expected for a Ca^{2+} induced conformational transition in which the environment of the Trp side chain becomes more nonpolar, more chiral, and less accessible to solvent, observations fully consistent with the known environment of residue 154 in the crystal structure of the $2Ca^{2+}$ state.

One of the more striking aspects of the present observations is the difference in the spectral features of F154W in the presence of Ca^{2+} versus Mg^{2+}. In the fluorescence emission spectrum (Figure 2A) it can be seen that the quantum yield is increased from 0.092 to 0.120 when 2 mM Ca^{2+} is replaced by 40 mM $MgCl_2$. This is not an ionic strength effect since the emission spectrum in 40 mM $MgCl_2$ plus 2 mM $CaCl_2$ is superimposable upon that in 2 mM $CaCl_2$ alone. This is explicable of course in terms of the displacement of Mg^{2+} cations by Ca^{2+} ions even when the $MgCl_2$ concentration is

at this high level and is consistent with the reported affinities of sites III/IV for Ca^{2+} and Mg^{2+} (see review by Leavis & Gergely (1984)). The fact that the fluorescence emission spectra of the protein in Ca^{2+} and in Ca^{2+} plus Mg^{2+} are superimposable also shows that the two additional and very low affinity Mg^{2+} binding sites ($K_a \cong 10^2$ M^{-1}), which are noncompetitive with Ca^{2+} (originally described by Potter and Gergely 1975)), have no effect on the fluorescence properties of F154W when saturated with Ca^{2+}. This was also true for the N domain spectral probe mutant F29W, whose fluorescence emission spectrum was not altered by Mg^{2+} concentrations as high as 46 mM in the absence of Ca^{2+} (Pearlstone et al., 1992).

Similar differences in the effects of Ca^{2+} versus Mg^{2+} on the spectral features of F154W are seen in the UV absorbance difference spectra, in the near UV CD spectra (Figure 3), and in the acrylamide quenching data (Figure 4). These all suggest that the environment of Trp-154 is not the same in the Ca^{2+} and Mg^{2+} states of F154W and that the structures of the C domain are different depending on whether Ca^{2+} or Mg^{2+} fills its sites III/IV. These observations are consistent with most other reports of structural comparisons of these two states. While some investigators (Seamon et al., 1977; Drakenberg et al., 1987) have reported the absence of significant differences in the conformations of the two forms, the weight of evidence points in the opposite direction. Thus, based on proton magnetic resonance observations, several reports (Levine et al., 1978; Drabikowski et al., 1985; Tsuda et al., 1988, 1990) have concluded that while the overall conformational fold of the C domain is similar in the Mg^{2+} and Ca^{2+} bound states, differences are seen in a number of resonances including those corresponding to the aromatic Phe cluster. This view has more recently been reinforced by Fourier transform infrared spectroscopy measurements (Trewhella et al., 1989) in which the metal-induced changes in the conformationally sensitive amide I′ bands were observed to be quite different for Mg^{2+} and Ca^{2+}. In the case of the primary EF site of pike 4.10 parvalbumin, X-ray structure determinations have now shown that the substitution of Ca^{2+} (unhydrated ionic radius 0.99 Å) by Mg^{2+} (unhydrated ionic radius 0.64 Å) is accompanied by a contraction of the coordination sphere (Declercq et al., 1991). A decrease in the mean oxygen metal distance by a value of 0.25 Å and a change from a coordination number of 7 to 6 was observed. This was associated with a change, among others, in the invariant bidentate ligand nature of Glu-101 (an invariant residue at position 12 of the Ca^{2+} binding loops of EF hand proteins) to that of a monodentate ligand. Such a transition to accommodate either Ca^{2+} or Mg^{2+} and involving rotation about the side chain torsion angles of this invariant Glu had previously been predicted by Strynadka & James (1989). The present observations of an alteration in the environment of Trp-154 of the TnC mutant F154W when Mg^{2+} replaces Ca^{2+} in sites III/IV are certainly consistent with such a mechanism in the C domain of this protein.

In the present work the potential application of the fluorescence properties of F154W for studies of the interaction of TnC with the inhibitory peptides of troponin I has been explored under different ionic conditions. Addition of Ip1 to a final concentration of 19 μM (5-fold excess) in the presence of 2 mM $CaCl_2$ led to a significant increase in relative fluorescence and a small shift in λ_{max} of fluorescence emission (see Figure 2B). No such change in fluorescence upon the addition of Ip1 was observed in the absence of divalent metal nor in the presence of Mg^{2+}. The absence of such Ip1 induced fluorescence changes for the apo and $2Mg^{2+}$ states indicates that even though Ip binding does occur with these forms of the protein (see later discussion), the environment of Trp-154 is not affected. Taking advantage of this inhibitory peptide induced and Ca^{2+} specific fluorescence change, it has been possible to measure and compare the binding affinities of three different forms of the inhibitory region of TnI to the $4Ca^{2+}$ state of TnC. The smallest of these, Ip3 (residues 104–115), has previously been shown to represent the minimal sequence of the inhibitory region of troponin I necessary for full inhibition of actomyosin S1 ATPase activity. Peptide Ip2 (residues 104–116) has the additional Met at residue 116 and lacks the amide group while the longest peptide Ip1 (residues 96–116) is neither acetylated nor amidated. The binding data (Figure 5) show that the presence of an additional Met at residue 116 of Ip2 and an ionized α-COO^- group does not appear to have a significant effect on binding. The binding affinities of Ip2 and Ip3 are very similar. A lengthening of the inhibitory peptide by eight residues in the NH_2-terminal direction as in Ip1 on the other hand increases the binding affinity 8-fold to $K_a = 5.0\ (\pm 0.9) \times 10^5$ M^{-1}. It is clear that although residues 104–115 may represent the minimal sequence necessary for inhibition of actomyosin ATPase, those residues 96–103 of the extended Ip1 inhibitory peptide (residues 96–116) make a substantial contribution to its binding affinity with TnC. That the inhibitory region of troponin I at the interface with TnC may also extend in the COOH-terminal direction to residue 121 and perhaps beyond is indicated by the cross-linking studies of Dobrovol'sky et al. (1984), Leszyk et al. (1990), and Kobayashi et al. (1991).

Present evidence (reviewed by Grabarek et al. (1992)) strongly indicates that both domains of TnC are involved in interaction with the inhibitory region of troponin I. Thus by a variety of approaches including fragment studies (Weeks & Perry, 1978; Grabarek et al., 1981), ^1H NMR (Dalgarno et al., 1982), and cross-linking by a photoactivable benzophenone or zero-length cross-linking (Leszyk et al., 1987, 1988, 1990; Wang et al., 1990; Kobayashi et al., 1991), peptide regions of both domains have been implicated in such interaction. These have included (using chicken TnC sequence numbers) residues 92–103 (E helix) of the C domain and residues 49–81 of the N domain. Together with other considerations, these observations have suggested that, in its interaction with TnI, TnC may adopt a compact structure similar to that seen with calmodulin in its complex with the 26-residue peptide of the calmodulin binding domain of myosin light chain kinase (Ikura et al., 1992).

In the present study, our observations indicate that the primary site of interaction of Ip1 (residues 96–116 of TnI) is with the C domain. Thus, at a molar ratio of 5:1 of Ip1 peptide to F29W or rTnC, there was a very significant increase in calcium affinity of the C domain (see Figure 1) but little change in that of the N domain as monitored by the Ca^{2+} titrations of the far UV CD ellipticity at 221 nm. This Ip1-induced increase in Ca^{2+} affinity of the C domain was also seen in the fluorescence measurements of F154W (Figure 1B). These observations indicate that, at the concentrations used in the far UV CD titration of Figure 1A (i.e., 175 μM Ip1 and 35 μM rTnC or F154W), binding of Ip1 is occurring primarily at a site on the C domain. Further, this C domain binding has little effect on the Ca^{2+} affinity of the N domain. This latter observation and interpretation are in disagreement with those recently reported by Van Eyk et al. (1991) but are consistent with those of Lan et al. (1989), who have also concluded that the strongest binding for the inhibitory peptide (residues 104–115 in their case) is with the C domain of TnC.

The present data are also consistent with a ^{19}F NMR study (Campbell et al., 1991) in which titration curves of Ca^{2+}-saturated TnC with N^{α}-acetyl [^{19}FPhe106] TnI (104–115) amide could be fitted either to a 1:1 binding model or to a 2:1 model in which the binding affinity for the second peptide binding site is 10–20-fold weaker than for the first site. Slupsky et al. (1992) have also recently shown by ^1H NMR that the binding of Ip3 is associated with perturbations of chemical shifts of a number of residues in the C domain with minimal effect on the N domain at the molar ratios used in their work. Recent studies in our laboratory of the interaction of inhibitory peptides with F29W and F105W mutants of intact rTnC and isolated C and N domains are also in agreement with these interpretations (manuscript in preparation) and demonstrate that, at high molar ratios of inhibitory peptide to protein, binding occurs with both N and C domains, resulting in increased Ca^{2+} affinity of both domains.

Pertinent to this discussion are the recent observations of Swenson and Fredricksen (1992), who have compared the binding of a Trp-labeled inhibitory peptide (residues 103–115 with Trp at 103) to rabbit skeletal TnC and its two fragments, residues 1–97 and 98–159, derived by chemical cleavage at Cys-98. Their results indicate a 4-fold-stronger binding to the N fragment as compared with C fragment (binding constants of 2.5×10^5 and 0.65×10^5 M^{-1}, respectively). Since their site of cleavage at peptide bond 97–98 is in the region (residues 88–100 of rabbit TnC) identified by many as a major site for interaction with the inhibitory region of TnI, their N fragment contains not only the N domain Ip binding sequence (residues 46–78) but also a significant segment of the E helix Ip binding region, normally considered as part of the C domain. As appreciated by the authors it is not surprising, therefore, that the relative binding affinities of Ip for N and C domains are reversed from those observed in the present and other studies in which these two binding regions are intact.

One of the more significant observations in the present work is the Ca^{2+} dependency of the fluorescence change induced by Ip binding. No such change is observed in the absence of divalent ions nor in the presence of Mg^{2+} but absence of Ca^{2+}. This is not due to a lack of binding since the cumulative data of Katayama and Nozaki (1982), Van Eyk and Hodges (1987, 1988), Swenson and Fredricksen (1992), and Tsuda et al. (1992) show that Ip binding to TnC occurs with both the apo and $2Mg^{2+}$ states of TnC. Taking the binding constants of Swenson & Fredricksen (1992) for TnC and their Ip peptide (residues 103–115 in which residue 103 is Trp), it can be calculated that, at the concentrations used in the present work, F154W would be 91%, 56%, and 65% saturated with Ip1 in the $4Ca^{2+}$, $2Mg^{2+}$, and apo states, respectively. We must conclude, therefore, that the fluorescence spectral change induced by Ip1 binding occurs only with the $4Ca^{2+}$ state of the protein and not with the $2Mg^{2+}$ or apo states. This together with the different binding affinities reported by others (Swenson & Fredricksen, 1992; Tsuda et al., 1992) for the apo, Mg^{2+}, and Ca^{2+} states strongly implies that the structural interface at the interaction site of Ip with the C domain of TnC is not the same for the Ca^{2+} and Mg^{2+} states of the protein.

In summary, it has been shown that the mutation of Phe-154 to Trp has no significant effects on the overall secondary structure of the protein, nor on its ability to function in the Ca^{2+} regulation of the reconstituted troponin–tropomyosin–actomyosin S1 ATPase system. The 2-fold decrease in Ca^{2+} binding affinity of the C domain sites III/IV can be rationalized in terms of the largely disordered apo state of the C domain and the known crystal structure of this domain in the $2Ca^{2+}$ state. Several spectral features including acrylamide fluorescence quenching indicate a structural difference between the Ca^{2+} and Mg^{2+} filled states of the C domain. Binding of the extended inhibitory peptide Ip1 (residues 96–116) of troponin I is increased ~8-fold over that of Ip2 (residues 104–116) or Ip3 (residues 104–115) and is of higher affinity for C domain than for N domain. The Ca^{2+} dependence of Ip induced fluorescence changes, not observed in the presence of Mg^{2+}, nor in the absence of Ca^{2+}/Mg^{2+}, implies a difference in the structural interface between the Ca^{2+}, Mg^{2+}, and apo states of the C domain of the F154W protein and the inhibitory peptides.

ACKNOWLEDGMENT

We thank Mrs. Linda Weiner and Mr. Pierre Dubord for their skilled assistance in the preparation of proteins.

REFERENCES

Campbell, A. P., Cachia, P. J., & Sykes, B. D. (1991) *Biochem. Cell Biol. 69*, 674–681.
Chong, P. C. S., & Hodges, R. S. (1981) *J. Biol. Chem. 256*, 5064–5070.
Dalgarno, D. C., Grand, R. J. A., Levine, B. A., et al. (1982) *FEBS Lett. 150*, 54–58.
Declercq, J.-P., Tinant, B., Parello, J., & Rambaud, J. (1991) *J. Mol. Biol. 220*, 1017–1039.
Dobrovol'sky, A. B., Gusev, N. B., & Friedrich, P. (1984) *Biochim. Biophys. Acta 789*, 144–151.
Drabikowski, W., Dalgarno, D. C., Levine, B. A., et al. (1985) *Eur. J. Biochem. 151*, 17–28.
Drakenberg, T., Forsen, S., Thulin, E., & Vogel, H. J. (1987) *J. Biol. Chem. 262*, 672–678.
Eftink, M. R., & Ghiron, C. A. (1976) *Biochemistry 15*, 672–680.
Fabiato, A. (1988) *Methods Enzymol. 157*, 378–417.
Golosinska, K., Pearlstone, J. R., Borgford, T., et al. (1991) *J. Biol. Chem. 290*, 3770–3775.
Grabarek, Z., Drabikowsky, W., Leavis, P. C., et al. (1981) *J. Biol. Chem. 256*, 13121–13127.
Grabarek, Z., Tao, T., & Gergely, J. (1992) *J. Muscle Res. Cell Motil. 13*, 383–393.
Heinonen, J. K., & Lahti, R. J. (1981) *Anal. Biochem. 113*, 313–317.
Herzberg, O., & James, M. N. G. (1985a) *Nature 313*, 653–659.
Herzberg, O., & James, M. N. G. (1985b) *Biochemistry 24*, 5298–5302.
Herzberg, O., & James, M. N. G. (1988) *J. Mol. Biol. 203*, 761–768.
Herzberg, O., Moult, J., & James, M. N. G. (1986) *J. Biol. Chem. 261*, 2638–2644.
Ho, S. N., Hunt, H. D., Horton, R. M., et al. (1989) *Gene 77*, 51–59.
Ikura, M., Clore, G. M., Gronenborn, A. M., et al. (1992) *Science 256*, 632–638.
Johnson, J. D., & Potter (1978) *J. Biol. Chem. 253*, 3775–3777.
Katayama, A., & Nozaki, S. (1982) *J. Biochem. 91*, 1449–1452.
Kobayashi, T., Tao, T., Grabarek, Z., et al. (1991) *J. Biol. Chem. 266*, 13746–13751.
Lan, J., Albaugh, S., & Steiner, R. F. (1989) *Biochemistry 28*, 7380–7385.
Leavis, P. C., & Gergely, J. (1984) *Crit. Rev. Biochem. 16*, 235–305.
Leszyk, J., Collins, J. H., Leavis, P. C., & Tao, T. (1987) *Biochemistry 26*, 7042–7047.
Leszyk, J., Collins, J. H., Leavis, P. C., & Tao, T. (1988) *Biochemistry 27*, 6983–6987.

Leszyk, J., Grabarek, Z., Gergely, J., & Collins, J. H. (1990) *Biochemistry 29*, 299–304.
Levine, B. A., Thornton, J. M., Fernandes, R., et al. (1978) *Biochim. Biophys. Acta 535*, 11–24.
Li, M. X., Chandra, M., Pearlstone, J. R., et al. (1994) *Biochemistry*, in press.
Mak, A. S., Golosinska, K., & Smillie, L. B. (1983) *J. Biol. Chem. 258*, 14330–14334.
McCubbin, W. D., Oikawa, K., Sykes, B. D., & Kay, C. M. (1982) *Biochemistry 21*, 5948–5956.
Mead, D. A., Skorupa, E. S., & Kemper, B. (1986) *Protein Eng. 1*, 67–74.
Pearlstone, J. R., Borgford, T., Chandra, M., et al. (1992) *Biochemistry 31*, 6545–6553.
Potter, J. D., & Gergely, J. (1975) *J. Biol. Chem. 250*, 4628–4633.
Reinach, F. C., & Karlsson, R. (1988) *J. Biol. Chem. 263*, 2371–2376.
Satyshur, K. A., Rao, S. T., Pryzalska, D., et al. (1988) *J. Biol. Chem. 263*, 1628–1647.
Seamon, K. B., Hartshorne, D. J., & Bothner-By, A. A. (1977) *Biochemistry 16*, 4039–4046.
Slupsky, C. M., Shaw, G. S., Campbell, A. P., & Sykes, B. D. (1992) *Protein Science 1*, 1595–1603.
Smillie, L. B. (1982) *Methods Enzymol. 85*, 234–241.
Spudich, J. A., & Watts, S. (1971) *J. Biol. Chem. 246*, 4866–4871.
Strynadka, N. C. J., & James, M. N. G. (1989) *Annu. Rev. Biochem. 58*, 951–998.
Sundaralingam, M., Bergstrom, R., Strasburg, G., et al. (1985) *Science 227*, 945–948.
Swenson, C. A., & Fredricksen, R. S. (1992) *Biochemistry 31*, 3420–3429.
Tobacman, L. S. (1987) *Biochemistry 26*, 492–497.
Tobacman, L. S., & Lee, R. (1987) *J. Biol. Chem. 262*, 4059–4064.
Trewhella, J., Liddle, W. K., Heidorn, D. B., & Strynadka, N. C. J. (1989) *Biochemistry 28*, 1294–1301.
Trigo-Gonzalez, G., Racher, K., Burtnick, L., & Borgford, T. (1992) *Biochemistry 31*, 7009–7015.
Tsuda, S., Hasegawa, Y., Yoshida, M., et al. (1988) *Biochemistry 27*, 4120–4126.
Tsuda, S., Ogura, K., Hasegawa, Y., et al. (1990) *Biochemistry 29*, 4951–4958.
Tsuda, S., Aimoto, S., & Hikichi, K. (1992) *J. Biochem. 112*, 665–670.
Van Eyk, J. E., & Hodges, R. S. (1987) *Biochem. Cell Biol. 65*, 982–988.
Van Eyk, J. E., & Hodges, R. S. (1988) *J. Biol. Chem. 263*, 1726–1732.
Van Eyk, J. E., Kay, C. M., & Hodges, R. S. (1991) *Biochemistry 30*, 9974–9981.
Wang, Z., Sarkar, S., Gergely, J., & Tao, T. (1990) *J. Biol. Chem. 265*, 4953–4957.
Weeds, A. G., & Taylor, R. S. (1975) *Nature 257*, 54–56.
Weeks, R. A., & Perry, S. V. (1978) *Biochem. J. 173*, 449–457.
Wilkinson, J. M., & Grand, R. J. A. (1978) *Nature 271*, 31–35.
Williams, T. C., Shelling, J. G., & Sykes, B. D. (1985) in *Nato Advanced Study Institute on NMR in the Life Sciences* (Bradbury, E. M., & Nicolini, C., Eds.) pp 93–103, Plenum Press, New York.
Zot, A. S., & Potter, J. D. (1987) *Annu. Rev. Biophys. Biochem. 16*, 535–559.